Clinical characteristics of peripapillary hyperreflective ovoid mass-like structures in myopic children

Lu Zhang[1], Zuo–Hui–Zi Yi[2], Xuan Jiang[1], Gong–Peng Sun[2], Fang Zhao[1], Li Zhang[1], Yi Xiang[1], Chang–Zheng Chen[2]

[1]Department of Ophthalmology, the Central Hospital of Wuhan, Tongji Medical College, Huazhong University of Science and Technology, Wuhan 430014, Hubei Province, China

[2]Eye Center, Renmin Hospital of Wuhan University, Wuhan 430060, Hubei Province, China

Correspondence to: Yi Xiang. Department of Ophthalmology, the Central Hospital of Wuhan, Tongji Medical College, Huazhong University of Science and Technology, Wuhan 430014, Hubei Province, China; Chang-Zheng Chen. Eye Center, Renmin Hospital of Wuhan University, No. 9 Zhang Zhi Dong Street, Wuchang District, Wuhan 430060, Hubei Province, China. whuchenchzh@163.com
Received: 2023-11-10   Accepted: 2024-04-01

Abstract

● **AIM:** To describe the characteristics of peripapillary hyperreflective ovoid mass-like structure (PHOMS) in myopic children and to investigate factors associated with PHOMS.

● **METHODS:** This retrospective observational study included 101 eyes of 101 children (age ≤17y) with myopia. All included patients underwent comprehensive clinical examination. Optic nerve canal parameters, including disc diameter, optic nerve head (ONH) tilt angle, and border tissue angle were measured using serial enhanced-depth imaging spectral-domain optical coherence tomography (EDI-OCT). Based on the optic disc drusen consortium's definition of PHOMS, eyes were classified as PHOMS group and non-PHOMS group. PHOMS was categorized according to height.

● **RESULTS:** Sixty-seven (66.3%) eyes were found with PHOMS. Small PHOMS could only be detected by optical coherence tomography (OCT). Medium PHOMS could be seen with blurred optic disc borders corresponding to OCT. The most frequent location of PHOMS was at the nasosuperior (91%, 61 of 67 eyes) to ONH disc. The axial length and spherical equivalent were more myopic in the PHOMS group than in the non-PHOMS group (both $P<0.001$). ONH tilt angle was also significantly greater in PHOMS group than in non-PHOMS group [8.90 (7.16-10.54) *vs* 3.93 (3.09-5.25), $P<0.001$]. Border tissue angle was significantly smaller in PHOMS group than in non-PHOMS-group [29.70 (20.90-43.81) *vs* 45.62 (35.18-60.45), $P<0.001$]. In the multivariable analysis, spherical equivalent (OR=3.246, 95%CI=1.209-8.718, $P=0.019$) and ONH tilt angle (OR=3.275, 95%CI=1.422-7.542, $P=0.005$) were significantly correlated with PHOMS. There was no disc diameter associated with PHOMS. In the linear regression analysis, border tissue angle was negatively associated with PHOMS height (β=-2.227, $P<0.001$).

● **CONCLUSION:** PHOMS is associated with optic disc tilt and optic disc nasal shift in myopia. Disc diameter is not a risk factor for PHOMS. The changes in ONH caused by axial elongation facilitated an understanding of the mechanism of PHOMS.

● **KEYWORDS:** peripapillary hyperreflective ovoid mass-like structure; myopia; optic disc edema; enhanced-depth imaging spectral-domain optical coherence tomography

INTRODUCTION

In 2018, the Optic Disc Drusen Studies Consortium proposed a new enhanced-depth imaging spectral-domain optical coherence tomography (EDI-OCT) term: peripapillary hyperreflective ovoid mass-like structure (PHOMS)[1]. PHOMS, an oval-shaped mass-like structure, is located outside the optic disc above the opening of the bruch membrane opening (BMO) and is similar to the reflection of the retinal nerve fiber layer[1]. The presence of PHOMS encircling a segment of the optic disc results in indistinct margins and mimics genuine papilledema in pediatric patients[1]. To date, little was known about the exact pathogenesis of PHOMS. The histopathology of optic disc drusen (ODD) suggested that PHOMS might correspond to the lateral bulging or herniation of distended axons into the peripapillary retina[2].

Pediatric ophthalmology frequently received referrals of children with suspected optic papilledema. Eshun *et al*[3] reported that 51% (*n*=47) of patients with suspected papilledema were referred by optometrists. It has been shown that PHOMS was the most common cause of pseudo-papilledema in children[4]. There was currently no conclusive evidence as to whether PHOMS was congenital or acquired in children. Kim *et al*[5] guessed that PHOMS was an acquired formation rather than a congenital disease. Herein, we characterized and investigated the clinical features of PHOMS in myopic children. By analyzing the risk factors of PHOMS, we sought to identify the additional characteristics of the entity in myopia, which may shed new light on its pathogenesis.

SUBJECTS AND METHODS

Ethical Approval　The cross-sectional observation study protocol was approved by the institutional review board of the Central Hospital of Wuhan and Renmin Hospital of Wuhan University, and this study was performed by the Declaration of Helsinki [yuan-nei-lun-2021(4)]. All participants were informed about the study and signed informed consent was obtained from their guardians.

Participants　Children with myopia who visited these two hospitals for prescription and treatment of myopia from January to May 2022 were involved in this study. This study included children (age ≤17y) who had a best-corrected visual acuity of 20/20 or better in each eye and spherical equivalent (SE; spherical refraction plus half negative cylinder) of -0.5 diopters (D) or less. Astigmatism was between +2.0 and -2.0 D. Intraocular pressure (IOP) measured by non-contact tonometer was less than 21 mm Hg with bilateral IOP difference <5 mm Hg. None had any history or showed any evidence of significant ocular disease or ocular surgery. The exclusion criteria were a history of intraocular surgery and the presence of any ocular or systemic diseases. Whenever both eyes were eligible for inclusion, the right eye was selected for analysis.

All children underwent complete ophthalmic examinations including best-corrected visual acuity measurement, IOP measurement applanation tonometry, slit-lamp examination, refraction error, measurement of axial length (AL; IOL Master 500, Carl Zeiss Meditec, Germany), fundus photography (CR-2; canon, Japan), and EDI-OCT (Heidelberg Engineering, Heidelberg, Germany). Refractive error was quantified as SE. AL measurements were averaged five times using an IOL-Master 500. All patients' fundus images and EDI-OCT were performed by the same experienced operator (Zhang L).

Imaging Acquisition for Enhanced-Depth Imaging Spectral-Domain Optical Coherence Tomography　Two scanning protocols were used. The EDI-OCT scan was obtained using a 24-radial line B-scan centered on the optic disc, each at an angle of 7.5°. In a rectangle of 15°×15° or 15°×10°, we obtained horizontal and vertical scans centred on the optic disc that included the parapapillary region and the optic disc. The number of these automatic real-time repeat scans was set to an average of 20 images. Optical coherence tomography (OCT) images were adjusted to 1:1 μm before measurement using Image J (V1.53). The exclusion criteria were as follows: poor-quality images for more than 6 sections of 24 radial line B-scan disc scans. The optic disc was divided into four quadrants by its centre, nasosuperior, nasoinferior, tempoinferior, and temposuperior. Afterwards, the precise distribution of PHOMS out of 24 possible peripapillary locations was reassessed by the radial OCT scans. If the line connecting the two end clock positions of PHOMS was parallel to the long disc axis, it was recorded as the same direction of rotation of the optic disc.

Measurement of Deep Optic Nerve Head Parameters with EDI-OCT　BMO plane was regarded as the region between the terminations of Bruch's membrane at the optic nerve head (ONH)[6]. The distance between the two BMO points was defined as disc diameter. BMO diameter was measured by two graders (Zhang L and Sun GP), as the mean of minimum radial measurement and maximum radial measurement. The intersection of the shortest diameter of the optic disc and the longest diameter of the optic disc was the center of the optic disc. With myopic changes, the border tissue of Elschnig was extended externally and observed on OCT. Reis *et al*[7] defined this type of border tissue as externally oblique border tissue (EOBT). EOBT length was defined as the length between the end points of the EOBT tissue. Optic canal plane was defined as the line connecting the nasal BMO and the innermost margin of the temporal EOBT. ONH tilt angle was defined as the angle between the BMO plane and the optic canal plane at the maximum tilt location[8]. The angle between the BMO plane and the EOBT was defined as the border tissue angle (BTA). PHOMS height was vertically measured perpendicular to the retinal pigment epithelium layer by the plane of the maximum value in a cube center in the optic nerve. Based on these measurements, PHOMS was categorized as small (<300 μm), medium (300-500 μm) and large (≥500 μm)[9] (Figure 1). The maximum values of these parameters except disc diameter were used as ONH parameters in all analyses.

All images were assessed by two independent observers (Zhang L and Sun GP). Each independent observer was masked to both the participants' information and the chronological order of the photographs, and evaluated the blurring of optic disc boundaries and measured the optic disc parameters. To evaluate the interobserver reproducibility of measurements of the ONH parameters, 30 disc images were randomly selected.
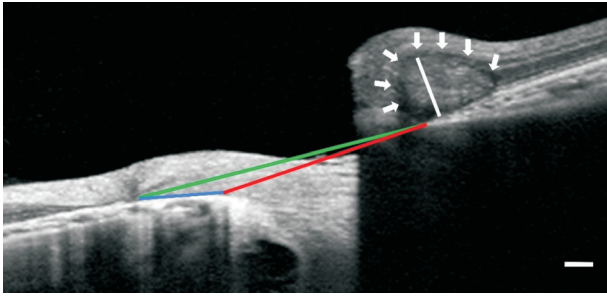
Figure 1 Measurement of parameters in a horizontal B-scan optical coherence tomography The nasal and temporal BMO points were defined based on the BMO reference plane (green line). The length from the temporal margin of the BMO to the border tissue scleral end was defined as the EOBT length (blue line). The angle between the green line and the blue line was defined as the BTA. The angle between the green line and the red line was defined as the optic nerve head tilt angle. PHOMS was marked with a white arrow. PHOMS height was shown by a white line. BTA: Border tissue angle; BMO: Bruch membrane opening; EOBT: Externally oblique border tissue; PHOMS: Peripapillary hyperreflective ovoid mass-like structure; Scale bar: 200 μm.

Statistical Analysis All data were put into an Excel spreadsheet (Microsoft Corp, Redmond, WA, USA), and statistical analyses were performed using SPSS software version 18.0 (SPSS, Inc, Chicago, IL, USA). Intraclass correlation coefficients were calculated to evaluate the reliability between the ONH parameters measured by the two independent observers. The data conforming to the normal distribution were expressed as mean ± standard deviation. Data from the skewed distributions were expressed as medians and quartiles. The data normality was verified by the Shapiro-Wilk test and histogram, and the homogeneity of variances was verified by Levene's test. Normal distributions were analyzed using Student's t-test or one-way analysis of variance. Skewed distributions were compared using the Mann-Whitney U and Kruskal-Wallis tests.

To identify the factors associated with PHOMS and myopia, univariate and multivariate logistic regression analyses were used and the adjusted odds ratios (OR) with 95% confidence intervals (CI) were calculated. AL was not included in the multivariate analysis because of the high multicollinearity with SE.

Pearson or Spearman correlation analyses were used to identify relationships between quantitative features. Partial correlation analysis was performed when adjusting other variables to assess their correlations. Linear regressions were performed to assess the relationships between PHOMS height and BTA. $P<0.05$ was considered statistically significant.

RESULTS

Totally 101 participants (101 eyes) were enrolled in the study.

Sixty-seven (66.3%) were classified as the PHOMS present group and 34 (33.7%) eyes were in non-PHOMS group. Totally 56 patients (55.4%) were bilaterally affected. The median age and SE were 11y (range: 7-17y) and -2.63 D (range: -0.5 to -8 D), respectively. The demographic and clinical characteristics of the subjects were presented in Table 1.

Morphological Characteristics of PHOMS and ONH Small PHOMS can only be detected by OCT, and no sign of poorly defined optic disc boundaries was detected by fundus color photography (Figure 2). Medium PHOMS were seen with blurred optic disc borders. The vertical scans of the optic disc showed a deflection in the outer nuclear layer above the BMO and seemed to be connected to the nerve fiber layer at the edge of the optic disc. PHOMS had no back shadow and did not obscure the underlying tissue. Intraretinal fluid collections and ODD were not found in the three types of PHOMS (Figure 2). Twenty-six eyes (25.7%) showed exterior negative angulation (toward the sclera) of the peripapillary retinal pigment epithelial/Bruch membrane layer relative to the more peripheral peripapillary regions of the retina. None showed inward positive angulation (toward the vitreous) of the peripapillary retinal pigment epithelial/Bruch membrane layer. In the 67 eyes with PHOMS, the frequency of PHOMS were the nasosuperior (91%, 61 of 67 eyes), nasoinferior (86%, 58 of 67 eyes), the tempoinferior (13%, 9 of 67 eyes) and the temposuperior (0.1%, 5 of 67 eyes). In all of the eyes in PHOMS group, the position of PHOMS in the optic disc of 64 eyes was coincident with the direction of optic disc torsion (Figure 3).

Reliability of Optic Nerve Head Parameters The intraclass correlation coefficients of PHOMS height, BTA, ONH tilt angle, EOBT length, the smallest disc diameters, the largest disc diameters, and neuroretina height were 0.947 (95%CI: 0.894-0.975), 0.979 (95%CI: 0.967-0.992), 0.930 (95%CI: 0.859-0.966), 0.991 (95%CI: 0.984-0.996), 0.945 (95%CI: 0.885-0.973), 0.934 (95%CI: 0.864-0.967), and 0.993 (95%CI: 0.984-0.996), respectively (all $P<0.001$).

Analysis of Factors Associated with the Presence of PHOMS in Myopic Children Univariate analyses (Table 2) showed that PHOMS was significantly associated with age (OR: 1.333, 95%CI: 1.096-1.620, $P=0.004$), SE (OR: 4.2463.44, 95%CI: 2.320-7.769, $P<0.001$), BTA (OR: 0.951, 95%CI: 0.925-0.977, $P<0.001$), EOBT length (OR: 1.176, 95%CI: 1.100-1.257, $P<0.001$), disc diameter (OR: 0.751, 95%CI: 0.581-0.970, $P=0.029$), and ONH tilt angle (OR: 3.500, 95%CI: 2.070-5.918, $P<0.001$). In the multivariable analysis (Table 2), SE (OR: 3.246, 95%CI: 1.209-8.718, $P=0.019$) and ONH tilt angle (OR: 3.275, 95%CI: 1.422-7.542, $P=0.005$) remained significant in this model.

Table 1 Demographic and clinical characteristics

Variables	PHOMS (*n*=67)	Non-PHOMS (*n*=34)	*P*
Age (y)	12.00 (10.00-14.00)	10.00 (9.00-12.25)	0.002[a]
Male/female	24/43	19/15	0.054[b]
SE (D)	-3.25 (-4.0, -2.5)	-1.5 (-2.50, -1.0)	<0.001[a]
AL (mm)	25.03±0.93	24.38±0.85	<0.001[c]
Disc diameter (μm)	1614.19±150.16	1695.15±198.85	0.024[c]
EOBT length (μm)	395.00 (261.00-511.00)	149 (106.00-228.50)	<0.001[a]
ONH tilt angle (°)	8.90 (7.16-10.54)	3.93 (3.09-5.25)	<0.001[a]
BTA (°)	29.70 (20.90-43.81)	45.62 (35.18-60.45)	<0.001[a]
PHOMS height (μm)	290.43±9.51	-	-
RNFL-G (μm)	101.99±8.35	104.44±8.05	0.161[c]
RNFL-N (μm)	56.00 (46.00-62.00)	62.00 (52.25-69.25)	0.016[a]

SE: Spherical equivalent; BTA: Border tissue angle; EOBT: Externally oblique border tissue; RNFL-G: Retinal nerve fiber layer globe; RNFL-N: Retinal nerve fiber layer nasal; PHOMS: Peripapillary hyperreflective ovoid mass-like structure; D: Diopter. [a]Analyzed with the Mann-Whitney *U* test; [b]Analyzed with Chi-square test; [c]Analyzed with the Student *t*-test.

Table 2 Factors associated with the presence of PHOMS

Variables	Univariate Analysis			Multivariate Analysis[a]		
	OR	95%CI	*P*	OR	95%CI	*P*
Age	1.333	(1.096, 1.620)	0.004	0.912	(0.912, 1.338)	0.637
Male/female	0.441	(0.441, 1.022)	0.056	0.682	(0.108, 4.285)	0.683
SE	4.246	(2.320, 7.769)	0.001	3.246	(1.209, 8.718)	0.019
AL	2.373	(1.380, 4.079)	0.002	-	-	-
BTA	0.951	(0.925, 0.977)	0.001	0.982	(0.894, 1.079)	0.706
EOBT length	1.176	(1.100, 1.257)	0.001	1.068	(0.888, 1.285)	0.486
Disc diameter	0.751	(0.581, 0.970)	0.029	0.711	(0.401, 1.262)	0.244
ONH tilt angle	3.500	(2.070, 5.918)	0.001	3.275	(1.422, 7.542)	0.005

SE: Spherical equivalent; AL: Axial length; EOBT: Externally oblique border tissue; RNFL-G: Retinal nerve fiber layer globe; RNFL-N: Retinal nerve fiber layer nasal; BTA: Border tissue angle; EOBT: Externally oblique border tissue; PHOMS: Peripapillary hyperreflective ovoid mass-like structure; SE: Per 1 diopter decrease; EOBT: Per 10 μm increase; Disc diameter: Per 10 μm increase; BTA: Per 1 degree; ONH tilt angle: Per 1 degree. [a]All variables were adjusted. AL was not included in the multivariate analysis because of the high multicollinearity with spherical equivalent.

Table 3 Clinical features of small and medium PHOMS

Parameters	Small PHOMS (*n*=41)	Medium PHOMS (*n*=26)	*P*
Age (y)	11.56±2.48	12.85±1.99	0.030[a]
SE (D)	-3.0 (-3.63, -2.25)	-3.9 (-4.88, -2.63)	0.630[b]
AL (mm)	24.84±0.79	25.32±1.02	0.037[a]
Disc diameter (μm)	1627.81±137.19	1592.73±169.23	0.355[a]
EOBT length (μm)	319.00 (213.00, 433.50)	471.50 (390.25, 623.75)	<0.001[b]
ONH tilt angle (°)	8.41 (6.75, 10.35)	9.34 (7.75, 12.80)	0.127[b]
BTA (°)	40.57 (26.50, 51.87)	21.58 (16.60, 29.54)	0.001[b]
PHOMS height (μm)	248.00 (215.00, 276.00)	357.50 (331.00, 414.00)	0.001[b]
RNFL G (μm)	101.59±7.57	102.62±9.60	0.626[a]
RNFL N (μm)	56.00 (56.00, 63.50)	54.00 (44.50, 62.00)	0.440[b]

SE: Spherical equivalent; AL: Axial length; EOBT: Externally oblique border tissue; ONH: Optic nerve head; BTA: Border tissue angle; PHOMS: Peripapillary hyperreflective ovoid mass-like structure; RNFL-G: Retinal nerve fiber layer globe; RNFL-N: Retinal nerve fiber layer nasal; SE: Per 1 diopter decrease; EOBT: Per 10 μm increase; Disc diameter: Per 10 μm increase; BTA: Per 1 degree; ONH tilt angle: Per 1 degree. [a]Analyzed with independent-samples *t*-test. [b]Analyzed with Mann-Whitney *U* test.

Analysis of PHOMS Type Table 3 showed the characteristics of PHOMS in the two groups. EOBT length, BTA, retinal nerve fiber layer globe, and retinal nerve fiber layer nasal showed statistically significant differences between three
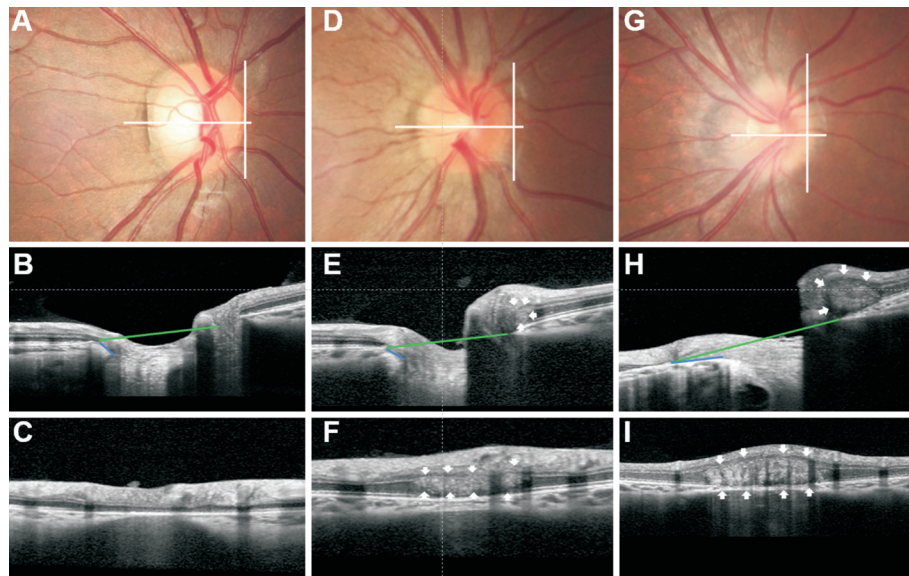
Figure 2 Fundus photography (A, D, G), OCT horizontal B-scan (B, E, H), and OCT vertical B-scan (C, F, I) of the normal, small, and medium PHOMS A, D and G were fundus pictures of normal fundus, small PHOMS, and medium PHOMS, respectively. B, E and H were OCT horizontal B-scans that pass through the center of the optic dis (horizontal white line of fundus photography). C, F and I were OCT vertical B-scans of the nasal border of the optic disc (vertical white lines of fundus photography). PHOMS was marked with a white arrow. The angle between the green line and the blue line was border tissue angle. The larger the PHOMS, the smaller the border tissue angle. OCT: Optical coherence tomography; PHOMS: Peripapillary hyperreflective ovoid mass-like structure.
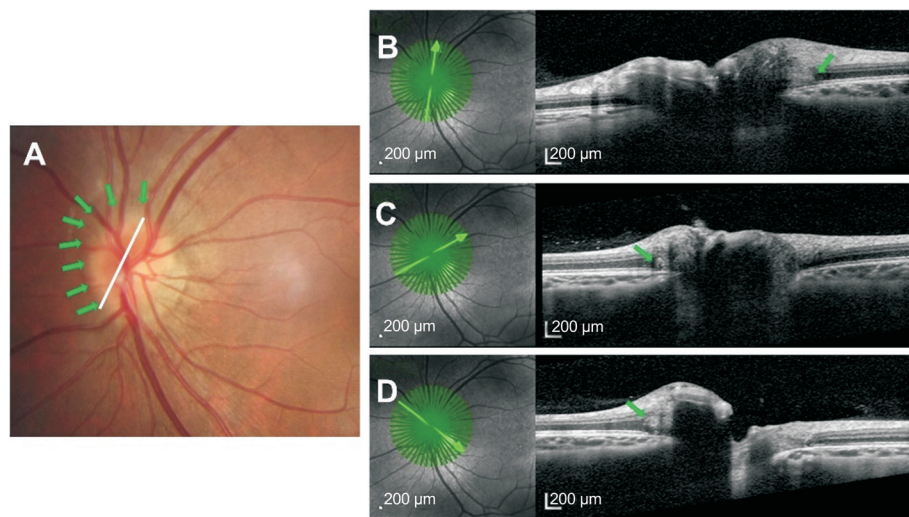

Figure 3 Configuration of the PHOMS on optical coherence tomography The line connecting the two end clock positions of PHOMS was parallel to the long disc axis in the left eye of an 8-year-old myopic child with PHOMS (visual acuity, 20/20). Blurred nasal optic disc were visible by fundus photogram (A). Optical coherence tomography line scan through the optic disc center (B, C, D) revealed PHOMS. According to the clockwise direction, the B plot showed the PHOMS end position, the C plot was the PHOMS start position, and the D plot was the highest PHOMS. PHOMS: Peripapillary hyperreflective ovoid mass-like structure.

groups ($P<0.05$, respectively). In the univariate analysis, age ($r=0.144$, $P=0.245$), disc diameter ($r=-0.093$, $P=0.456$), AL ($r=0.144$, $P=0.246$), ONH tilt angle ($r=0.211$, $P=0.087$), and SE ($r=-0.220$ $P=0.074$) were not significantly correlated with PHOMS height. BTA ($r=-0.497$, $P<0.001$) was negatively correlated with PHOMS height (Figure 4). EOBT length ($r=0.435$, $P<0.001$) was positively correlated with PHOMS height. In the linear regression analysis, BTA was significantly associated with PHOMS height ($\beta=-2.227$, $P<0.001$).

DISCUSSION

In this cross-sectional observational study, we investigated PHOMS features and related factors in myopic children. The principal findings of this study are as follows. First, the frequency of PHOMS was the nasosuperior (91%, 61 of 67 eyes). Second, disc diameter was not a risk factor for PHOMS. Third, PHOMS was also associated with optic disc nasal shift in myopia except for optic disc tilt.

Our study indicated that EDI-OCT was redounded to detect

small PHOMS with normal optic disc appearance. Small PHOMS was located only in the nasal juxtapapillary and was recommended to be detected by OCT. Medium PHOMS cause blurring of the optic disc border and should be differentiated from papilledema in myopic children. There was no significant difference in PHOMS between males and females[10-11]. Regardless of the size of the PHOMS, there was no positive angulation for the peripapillary retinal pigment epithelial/Bruch membrane layer. Kupersmith et al[12] reported in their study that 20 eyes (67%) had positive retinal pigment epithelial/Bruch membrane rim angles with papilledema. This clinical sign may be used to differentiate between PHOMS and papilledema.

PHOMS was first observed and described as "a boot-shaped" structures seen in spectral domain OCT B-scans of patients with ODD in 2011[13]. PHOMS was mistakenly interpreted as ODD in this study. Fraser et al[14] categorized PHOMS by etiology: disk edema-associated PHOMS, ODD-associated PHOMS, and anomalous disk-associated PHOMS. Anomalous disk-associated PHOMS includes tilted disc syndrome (TDS) and myopia. Pichi et al[15] found that 15 out of 38 eyes of pediatric patients with TDS exhibited a dome-shaped hyperreflective structure under vertical B-scan of ONH, consistent with the morphological features of herniated retinal nerve fibers. Our study showed that SE and ONH tilt angles were significantly correlated with PHOMS, in agreement with previous results[11]. It was believed that the nasal dragging of the lamina cribrosa as well as the stretching of the temporal sclera cause impingement and stress on optic nerve axons which lead to the occurrence of nasal PHOMS[16].

Intriguingly, the size of PHOMS was negatively correlated with BTA in our study. ONH shift towards nasal was supported by numerous previous studies[17]. Kim et al[18] found that the BTA became smaller and the length of the EOBT increased as the myopic shifted. It has been suggested that optic disc tilt should be considered as earlier myopic ONH changes[19]. Therefore, we speculated on the following process of PHOMS formation. First, as a result of the ONH tilt, the retinal nerve fiber appeared to be bent along the upper margin of the optic nerve head. Second, lateral force was more important in the progression of myopia as optic disc nasal shift with AL elongation. Consequently, optic disc nasal shift may be the main factor affecting the size of PHOMS after its formation. In this study, it was hypothesized that myopic optic disc tilt and optic disc nasal shift lead to laterally bulging of optic nerve fibers, which first accumulate on the nasal side of the optic disc. Our study showed the most frequent PHOMS were the nasosuperior (91%, 61 of 67 eyes). Most of the position of PHOMS in the optic disc (95.5%, 64 of 67 eyes) was coincident with the direction of optic disc torsion. Figure 5 shows
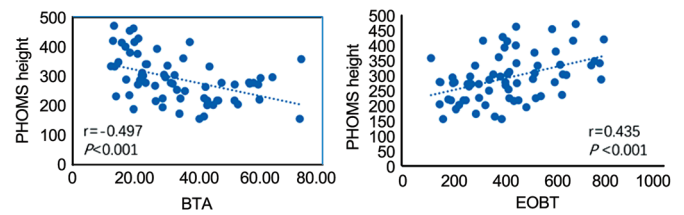

Figure 4 Univariate correlation analysis between PHOMS height and BTA, EOBT PHOMS: Peripapillary hyperreflective ovoid mass-like structure; BTA: Border tissue angle; EOBT: Externally oblique border tissue.
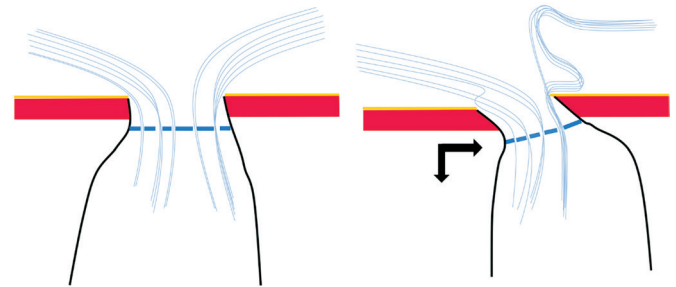

Figure 5 Schematic showing myopic optic nerve head changes and peripapillary hyperreflective ovoid mass-like structure formation during myopia progression As myopic shifts, the optic nerve head was tilted and shifted, resulting in the formation of peripapillary hyperreflective ovoid mass-like structure. The orange colour indicates Bruch membrane. The red color indicates choroid. The blue-dotted line indicates lamina cribrosa. The blue line indicates retinal nerve fiber. The black arrow indicates the direction of optic nerve head movement.

a schematic description of PHOMS formation and myopic ONH change. Certainly, this hypothesis needs to be further confirmed by longitudinal investigations in our future study.

East Asian children over the past few decades and will continue to be a leading. Myopia has become a major visual disorder among health issue with an annual incidence as high as 20%-30%[20]. According to the mammalian models of high myopia, scleral remodeling, which depends on the changes in the constitution of the scleral extracellular matrix (ECM), plays a significant part in the thinness of the sclera. Axial myopia was associated with posterior scleral deformity and optic nerve damage[21-23]. The reshaped optic disc may cause the optic nerve fibers to retain a state of high mechanical stress induced by stretching, while the deformation of the lamina cribrosa bends the axons of the nerve fibers as they pass through it and creates a shearing effect, which in turn injures the optic nerve fiber[24-25]. This may be one of the mechanisms of myopic neuropathy. Some studies demonstrated that PHOMS was an OCT marker of axoplasmic stasis in the optic nerve head[14,26]. Consequently, PHOMS as a morphological observation index may be an entry point for myopic optic neuropathy.

The present study suggested that optic disc diameter was not a risk factor of PHOMS in the multivariate analysis,

which was similar to a previous survey[11]. Lee *et al*[25] found a negative correlation between the height of buried ODD and the optic disc size and concluded that buried ODD was a precursor of visible ODD. The buried ODD in this study was exactly PHOMS based on the report from the Optic Disc Drusen Studies Consortium. Our study population was myopic children whereas the other study subjects had no age or myopia qualifiers[9]. Furthermore, the population included in other studies were children with blurred optic disc boundaries, so there was a greater chance of inclusion of medium and large PHOMS. However, there was no large PHOMS group in our study. Those differences may be related to study populations.

Strengths of our study include limiting the study population to children with axial myopia, excluding refractive myopia, and providing a precise analysis of optic disc changes as a result of AL changes. Second, the latest optic disc movement theory, optic disc nasal shift, was introduced to analyze its relationship with PHOMS. However, our study does have some limiting factors that should be considered. First, visual field was absent to clarify the clinical significance of PHOMS. Second, because this was a cross-sectional study, we can only report associations discovered without identifying causality. Third, no large PHOMS group in this study may be due to selection bias. Future studies that include more patients with large PHOMS would yield more conclusive results. Longitudinal follow-up is needed in the future to observe morphological changes in PHOMS due to increasing myopia. An animal model of myopia was established to obtain medium access to PHOMS pathology support.

In conclusion, this study investigated the clinical features of PHOMS and its correlation with myopia in children. This study was the first to demonstrate PHOMS was associated with optic disc nasal shift in myopia. The changes in ONH caused by axial elongation facilitate understanding the mechanism of PHOMS.

ACKNOWLEDGEMENTS

Conflicts of Interest: Zhang L, None; **Yi ZHZ,** None; **Jiang X,** None; **Sun GP,** None; **Zhao F,** None; **Zhang L,** None; **Xiang Y,** None; **Chen CZ,** None.

REFERENCES

1 Malmqvist L, Bursztyn L, Costello F, Digre K, Fraser JA, Fraser C, Katz B, Lawlor M, Petzold A, Sibony P, Warner J, Wegener M, Wong S, Hamann S. The optic disc drusen studies consortium recommendations for diagnosis of optic disc drusen using optical coherence tomography. *J Neuroophthalmol* 2018;38(3):299-307.

2 Tso MO. Pathology and pathogenesis of drusen of the optic nervehead. *Ophthalmology* 1981;88(10):1066-1080.

3 Eshun EL, Gwin JC, Ditta LC. Peripapillary hyperreflective ovoid masslike structures in a pediatric population referred for suspected papilledema. *J AAPOS* 2022;26(5):242.e1-242242.e6.

4 Flowers AM, Longmuir RA, Liu Y, Chen Q, Donahue SP. Variability within optic nerve optical coherence tomography measurements distinguishes papilledema from pseudopapilledema. *J Neuroophthalmol* 2021;41(4):496-503.

5 Kim MS, Hwang JM, Woo SJ. Long-term development and progression of peripapillary hyper-reflective ovoid mass-like structures: two case reports. *J Neuroophthalmol* 2022;42(1):e352-e355.

6 Aghsaei Fard M, Okhravi S, Moghimi S, Subramanian PS. Optic nerve head and macular optical coherence tomography measurements in papilledema compared with pseudopapilledema. *J Neuroophthalmol* 2019;39(1):28-34.

7 Reis ASC, Sharpe GP, Yang HL, Nicolela MT, Burgoyne CF, Chauhan BC. Optic disc margin anatomy in patients with glaucoma and normal controls with spectral domain optical coherence tomography. *Ophthalmology* 2012;119(4):738-747.

8 Han JC, Lee EJ, Kim SB, Kee C. The characteristics of deep optic nerve head morphology in myopic normal tension glaucoma. *Invest Ophthalmol Vis Sci* 2017;58(5):2695-2704.

9 Lee KM, Woo SJ, Hwang JM. Morphologic characteristics of optic nerve head drusen on spectral-domain optical coherence tomography. *Am J Ophthalmol* 2013;155(6):1139-1147.e1.

10 Ahn YJ, Park YY, Shin SY. Peripapillary hyperreflective ovoid mass-like structures (PHOMS) in children. *Eye (Lond)* 2022;36(3):533-539.

11 Lyu IJ, Park KA, Oh SY. Association between myopia and peripapillary hyperreflective ovoid mass-like structures in children. *Sci Rep* 2020;10(1):2238.

12 Kupersmith MJ, Sibony P, Mandel G, Durbin M, Kardon RH. Optical coherence tomography of the swollen optic nerve head: deformation of the peripapillary retinal pigment epithelium layer in papilledema. *Invest Ophthalmol Vis Sci* 2011;52(9):6558-6564.

13 Lee KM, Woo SJ, Hwang JM. Differentiation of optic nerve head drusen and optic disc edema with spectral-domain optical coherence tomography. *Ophthalmology* 2011;118(5):971-977.

14 Fraser JA, Sibony PA, Petzold A, Thaung C, Hamann S, ODDS Consortium. Peripapillary hyper-reflective ovoid mass-like structure (PHOMS):an optical coherence tomography marker of axoplasmic stasis in the optic nerve head. *J Neuroophthalmol* 2021;41(4):431-441.

15 Pichi F, Romano S, Villani E, Lembo A, Gilardoni F, Morara M, Ciardella AP, Ohno-Matsui K, Nucci P. Spectral-domain optical coherence tomography findings in pediatric tilted disc syndrome. *Graefes Arch Clin Exp Ophthalmol* 2014;252(10):1661-1667.

16 Meng LH, Yuan MZ, Zhao XY, Chen YX. Macular Bruch's membrane defects and other myopic lesions in high myopia. *Int J Ophthalmol* 2022;15(3):466-473.

17 Lee KM, Choung HK, Kim M, Oh S, Kim SH. Positional change of optic nerve head vasculature during axial elongation as evidence of lamina cribrosa shifting boramae myopia cohort study report 2. *Ophthalmology* 2018;125(8):1224-1233.

18 Kim M, Choung HK, Lee KM, Oh S, Kim SH. Longitudinal changes of optic nerve head and peripapillary structure during childhood myopia progression on OCT: boramae myopia cohort study report 1. *Ophthalmology* 2018;125(8):1215-1223.

19 Burgoyne CF, Wang YX, Jeoung JW, Hong S, Gardiner S, Reynaud J, Fortune B, Girard MJA, Sharpe G, Nicolela M, Chauhan BC, Yang HL. OCT optic nerve head morphology in myopia II: peri-neural canal scleral bowing and choroidal thickness in high myopia-an American ophthalmological society thesis. *Am J Ophthalmol* 2023;252:225-252.

20 Németh J, Daiki T, Dankovics G, Barna I, Limburg H, Nagy ZZ. Prevalence of refractive errors in Hungary reveals three-fold increase in myopia. *Int J Ophthalmol* 2022;15(7):1174-1179.

21 Morgan IG, Ohno-Matsui K, Saw SM. Myopia. *Lancet* 2012;379(9827):1739-1748.

22 Yu Q, Zhou JB. Scleral remodeling in myopia development. *Int J Ophthalmol* 2022;15(3):510-514.

23 Tang WQ, Luo YL, Wang XL, Duan XC. Changes of optic nerve head microcirculation in high myopia. *Int J Ophthalmol* 2023;16(1):102-107.

24 Ang M, Wong CW, Hoang QV, Cheung GCM, Lee SY, Chia A, Saw SM, Ohno-Matsui K, Schmetterer L. Imaging in myopia: potential biomarkers, current challenges and future developments. *Br J Ophthalmol* 2019;103(6):855-862.

25 Lee KM, Woo SJ, Hwang JM. Peripapillary hyperreflective ovoid mass-like structures: is it optic disc drusen or not? *J Neuroophthalmol* 2018;38(4):567-568.

26 Biousse V, Danesh-Meyer HV, Saindane AM, Lamirel C, Newman NJ. Imaging of the optic nerve: technological advances and future prospects. *Lancet Neurol* 2022;21(12):1135-1150.